

1  
2  
3  
4  
5  
6  
7  
8  
9  
10  
11  
12  
13  
14

# **Pilot-scale calcination of limestone in steam-rich gas for direct air capture**

*María Erans<sup>a,b</sup>, Seyed Ali Nabavi<sup>a</sup>, Vasilije Manović<sup>a\*</sup>*

<sup>a</sup> Power Engineering Centre, Cranfield University, Bedford, Bedfordshire, MK43 0AL, UK.

<sup>b</sup> Faculty of Engineering, University of Nottingham, Nottingham, NG7 2RD, UK.

\*Corresponding author: Vasilije Manović ([v.manovic@cranfield.ac.uk](mailto:v.manovic@cranfield.ac.uk))

15 **Abstract**

16 A novel polygeneration concept, which has been proposed recently, comprises a fuel-cell  
17 calciner integrated system in order to produce electricity and lime which can be used for direct  
18 air capture (DAC) to remove CO<sub>2</sub> from the atmosphere. However, the scalability of the  
19 integrated system needs to be further studied. In this work, calcination of limestone under  
20 steam-rich conditions simulating flue gas from a solid oxide fuel cell (SOFC), and subsequent  
21 ambient carbonation has been explored. Limestone was calcined under two steam  
22 concentration (21% and 35% vol) conditions in a 25 kW<sub>th</sub> pilot-scale bubbling fluidised bed  
23 (BFB), and then exposed to ambient air to evaluate DAC performance. Samples were  
24 characterised in order to quantify the hydration and carbonation conversions over time and,  
25 therefore, their DAC capacity. It was observed that steam reduces calcination time, confirming  
26 its catalytic effect, while the calcination temperature remained the same regardless of the steam  
27 composition at the same CO<sub>2</sub> partial pressure. Moreover, increasing steam concentration during  
28 calcination affected the material performance and DAC capacity at ambient conditions  
29 positively. Therefore, these findings demonstrate that limestone calcined under typical SOFC  
30 afterburner exhaust conditions is suitable as a DAC sorbent.

31

32

33 **Keywords:** calcination; steam; CO<sub>2</sub> capture; direct air capture; limestone

## 34 **1 Introduction**

35 In order to achieve the Paris Agreement target, reached at the 21<sup>st</sup> Conference of the UNFCC  
36 parties, of maintaining the mean global temperature rise below 2° C when compared to pre-  
37 industrial levels, a portfolio of technologies needs to be deployed [1]. These technologies  
38 include bioenergy with carbon capture and storage (BECCS) [2], direct air capture (DAC) and  
39 enhanced weathering of minerals, among others [3,4]. However, these carbon-negative  
40 technologies are still expensive and in early stages of development [5–8].

41 The reversible carbonation/calcination cyclic reaction of Ca-based materials (Eq. 1) has been  
42 widely researched for a variety of natural processes and applications such as production of  
43 cement, deployment in the iron and steel industry, water treatment, and desulphurisation. More  
44 recently, calcium looping (CaL) has been explored as a promising second-generation carbon  
45 capture technology, which employs the reaction of Ca-based materials with CO<sub>2</sub> [9]. It is aimed  
46 at the decarbonisation of large point sources such as power generation and industrial plants  
47 [10]. This technology comprises two interconnected fluidised beds and a Ca-based solid  
48 material being looped between the reactors. In the reactor called the carbonator, CaO reacts  
49 with the CO<sub>2</sub> present in a flue or fuel gas stream and forms calcium carbonate. The saturated  
50 sorbent is then circulated to another reactor (calciner) in order to regenerate sorbent at high  
51 temperature and to produce a concentrated CO<sub>2</sub> stream.



52 It has been suggested in several studies that injecting steam during carbonation and/or  
53 calcination has a positive effect on carbonation conversions over a number of  
54 capture/regeneration cycles at laboratory [11,12] and pilot plant scale [13]. Manovic and  
55 Anthony [14] investigated the effect of steam on carbonation for a variety of calcined  
56 limestones using a thermogravimetric analyser (TGA) and concluded that steam enhances  
57 sorbent conversion during the diffusion-controlled step (through the carbonate product layer).  
58 Donat et al. [11] also reported that steam injection during carbonation in a small bubbling

59 fluidised bed (BFB) raises carbonation conversion due to the minimisation of diffusion  
60 resistance. Further experiments were performed by Symonds et al. [15], which showed  
61 increased CO<sub>2</sub> capture capacity when steam (17% vol) was present in a BFB carbonator.  
62 With regard to the effect of steam addition during calcination, it has been typically considered  
63 as an effective method of lowering the sorbent decomposition temperature by means of  
64 reducing CO<sub>2</sub> partial pressure in the calciner [16]. Namely, it has been suggested that steam is  
65 adsorbed onto the CaO surface faster than CO<sub>2</sub>, which implies a weaker bond between CaO  
66 and CO<sub>2</sub>, thus, lowering the calcination temperature [17]. Also, experimental observations  
67 showed that the decomposition rates are more rapid when a small amount of steam was  
68 introduced in the calciner [18–20]. This phenomenon was initially linked to the enhancement  
69 of thermal conductivity in the calciner [20]. However, Wang et al. [17] hypothesised a catalytic  
70 effect of steam in CaCO<sub>3</sub> decomposition. Moreover, steam addition during calcination  
71 increases lime performance in the subsequent carbonation cycles [12,21,22]. It has been  
72 reported that porosity and surface area were reduced in the presence of steam [23]. This caused  
73 a shift towards larger pores when steam was present in the reactor, inducing steam-enhanced  
74 sintering, which led to a decrease of surface area and conversion [22–26]. Also, it has been  
75 reported that steam injection during calcination has a negligible effect on the subsequent  
76 carbonation when compared to steam injection during carbonation or carbonation and  
77 calcination simultaneously [27]. It has also been suggested that there is a synergistic effect  
78 when steam is introduced to both carbonator and calciner [12]. Donat et al. [11] indicated that  
79 the carbonation conversion was highest when steam was added to both carbonator and calciner,  
80 as opposed to injecting steam either during calcination or carbonation only.  
81 Recently, new concepts employing Ca-based sorbents have been explored, such as integration  
82 of CaL with concentrating solar power for thermochemical energy storage [28]. Industrial  
83 waste streams, such as carbide slag, have also been studied, and it has been experimentally

84 demonstrated that simultaneous CO<sub>2</sub> capture and thermochemical energy storage can be  
85 achieved [29]. Calcium hydroxide has been investigated as an efficient material for DAC  
86 processes; however, it requires high energy in order to regenerate [30]. Lime has also been  
87 suggested for DAC in a fluidised bed with solar energy used to provide heat needed for  
88 regeneration [31]. Moreover, the concept of simultaneous power generation and CO<sub>2</sub> capture  
89 from air using carbonate materials has recently been proposed [32]. In this process, the sorbent  
90 regeneration step is performed by using the high-grade heat from a solid oxide fuel cell (SOFC).  
91 SOFCs have been suggested for this process due to their high electrical efficiency [33–35], fuel  
92 flexibility [36–40], and ability to co-generate high grade heat [41]. A key advantage of SOFCs  
93 is that external reformer is not required in this technology [38]. The composition of the SOFC  
94 off-gas depends on the fuel supplied, but for natural gas comprises mainly CO<sub>2</sub> and steam [38].  
95 Then, steam is condensed, and concentrated CO<sub>2</sub> stream compressed, transported, and stored,  
96 typically in geological formations [4]. Therefore, the proposed process possesses several  
97 advantages, which include: generation of electricity and a concentrated CO<sub>2</sub> stream, as well as  
98 CO<sub>2</sub> capture from air using Ca-based materials at costs which are competitive compared to  
99 those of other DAC technologies [42]. This process has been demonstrated at laboratory scale  
100 using a 2 kWe SOFC with a fixed-bed calciner, showing promising performance [43]. In order  
101 to scale up the process, and explore the behaviour of the materials under realistic conditions, a  
102 fluidised bed calciner, such as employed in the CaL cycle technology, was perceived as a most  
103 suitable reactor choice.

104 In this work, calcination of limestone in steam-rich gas, simulating SOFC calciner conditions,  
105 is explored at BFB pilot-scale. The aim is to evaluate the technical feasibility of the SOFC  
106 calcination process and the effect of steam on calcination temperature and reaction time.  
107 Furthermore, the performance of the lime produced under realistic SOFC calciner process  
108 conditions, in order to be used for DAC, is tested. Finally, in addition to the practical

109 application of the proposed process, the fundamental aspects of the effect of steam on the  
110 performance of Ca-based materials in CO<sub>2</sub> capture processes are further explored. These are a  
111 key in order to evaluate potential of lime production under steam enriched conditions, such as  
112 those when the SOFC exhaust stream is used as a fuel and fluidizing gas.

## 113 **2 Experimental**

114 A detailed process diagram of the new concept for DAC by lime calcined using the high grade  
115 heat from SOFC is presented by Hanak et al. [32], and this study explores the calciner part of  
116 the integrated process. The experimental conditions during calcination were designed in order  
117 to simulate realistic gas composition from SOFC entering the calciner and conditions during  
118 combustion/calcination, primarily high concentration of steam. Finally, the DAC performance  
119 of limestone calcined under realistic conditions of the integrated process were tested by means  
120 of CO<sub>2</sub> capture from ambient air.

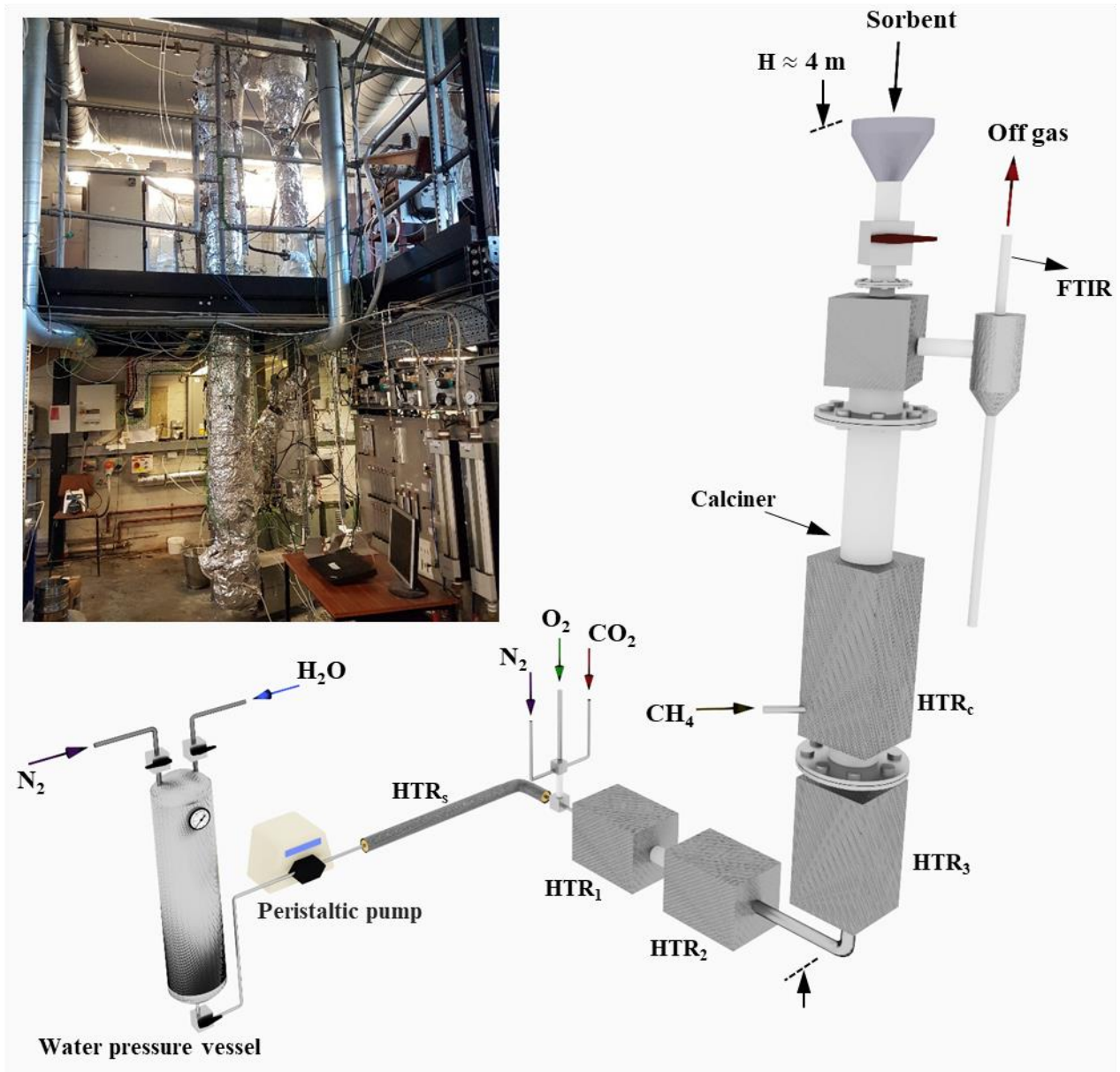
121

### 122 **2.1 Pilot-scale calciner description**

123 A 25 kW<sub>th</sub> pilot-scale bubbling fluidised bed (BFB) reactor was used for the calcination  
124 experiments. This calciner was redesigned CaL pilot plant [44] and similar in the size to the  
125 CaL pilot plant at INCAR-CSIC [45]. The set-up of the calciner is shown in a schematic manner  
126 in Figure 1. The calciner is 1.2 m high with an ID of 0.165 m and was operated at atmospheric  
127 pressure. The distributor plate comprised 20 nozzles of 6 1-mm holes each. The fluidising gas  
128 was heated by electrically-heated pipes and the calciner was additionally heated by electrical  
129 heater and combustion of natural gas inside the bed. The electrical heater was used for start-up  
130 of the calciner to heat it up to 600-650 °C, which was the temperature enabling ignition and  
131 stable combustion of natural gas. In order to calcine limestone under the conditions simulating  
132 combustion of the surplus fuel from SOFC anode, the further temperature increase was

133 achieved by combustion of natural gas. Therefore, during the calcination regime, the heat  
134 supply required for calcination was a combination of electrical heating and methane  
135 combustion, simulating combustion of unreacted fuel and high grade heat supply from SOFC.  
136 The steam introduced into the calciner was produced via an in-house steam generator consisting  
137 of a water pressure vessel at 2 bar, a peristaltic pump (Masterflex, Cole Parmer) to adjust the  
138 flow rates, and two 1.2 kW heating tapes (OMEGA, UK), operating at 400-500 °C. Prior to  
139 installing the heating tapes, the pipe was wrapped with mica tape to avoid any potential electric  
140 discharge. The other gases were supplied to the calciner and their flow rates were measured by  
141 rotameters. The off-gas concentrations were measured by a Fourier Transform Infrared  
142 analyser (FTIR, Protea, model FTPA-002). The temperature through the steam generation  
143 system was continuously monitored throughout the experiments by an in-house system using  
144 K-type thermocouples and an in-house controller.

145



146

147 Figure 1: Photograph (top left corner) and schematics of the pilot-scale BFB calciner. The  
 148 power of the calciner components are: preheaters (HTR<sub>1</sub> – 3 kW, HTR<sub>2</sub> – 3 kW, HTR<sub>3</sub> – 5  
 149 kW), steam line heating types (HTRs – 2 x 1.2 kW = 2.4 kW), calciner heater (HTR<sub>c</sub> – 8 kW),  
 150 and natural gas stream (9.6 L/min, CH<sub>4</sub> – ~3 kW).

151

## 152 2.2 Experimental procedure

153 Two sets of experiments were performed with different steam concentrations, while  
 154 maintaining the same fluidisation velocity (0.25 m/s) and CO<sub>2</sub> concentration (35% vol). The



155 calciner was first commissioned, and several tests were performed in order to ensure stable  
156 steam supply, avoiding condensation, and operation near to steady state. Then, two tests, with  
157 different steam concentrations (21% and 35% steam), were performed two times in order to  
158 ensure reproducibility of experimental conditions and measured results. Considering the  
159 accuracy of the measuring equipment and repeatability, it was estimated that relative error of  
160 the results presented in this study is in the range of  $\pm 5\%$ .

161 In the first instance, 13% vol steam was mixed with 29% CO<sub>2</sub>, and balanced with N<sub>2</sub>. The  
162 calciner was heated up to 700 °C, then the limestone was introduced into the vessel, and heated  
163 until the temperature reached 700 °C again. The inventory of the bed was kept the same for  
164 both experiments for consistency purposes, i.e., 3 kg of limestone per experiment. At that point,  
165 9.6 L/min of natural gas was fed into the calciner and combusted in 20.1 L/min O<sub>2</sub> in order to  
166 provide the necessary heat for the calcination. The steam and CO<sub>2</sub> concentrations at the outlet  
167 of the calciner, as measured by the FTIR, before calcination had started, were 21% and 35%  
168 vol, respectively, and this increase, compared to that at the inlet of the calciner, is a result of  
169 natural gas combustion ( $\text{CH}_4 + 2\text{O}_2 \rightarrow 2\text{H}_2\text{O} + \text{CO}_2$ ).

170 During the second experiment, 30% vol steam was mixed with 29% vol CO<sub>2</sub>, and balanced  
171 with N<sub>2</sub>. The flow rates of natural gas and O<sub>2</sub> were maintained the same as in the previous  
172 experiment in order to provide the same amount of heat for calcination. The steam and CO<sub>2</sub>  
173 concentrations at the outlet of the calciner, before calcination had started, were both 35% vol.  
174 When calcination was completed, i.e., when the CO<sub>2</sub> concentration at the outlet equalled the  
175 initial values before calcination, the calciner was cooled down using N<sub>2</sub> in order to avoid any  
176 carbonation and/or hydration of the already-calcined material.

177 It should be noted that gas composition in this study was selected assuming that the gas stream  
178 from SOFC anode with the excess of fuel is entering calciner. The model of the integrated  
179 process used to simulate the gas composition in calciner, considering the mass and heat

180 balance, is presented by Hanak et al. [32]. During the experiments, nitrogen was used to balance  
181 steam in order to mitigate risk of condensation in the reactor. The composition of the fluidising  
182 gas for both experiments is summarised in Table 1.

183 Table 1: Experimental gas concentrations

<b>Experiment</b>	<b>Steam (% vol)</b>	<b>CO<sub>2</sub> (% vol)</b>	<b>N<sub>2</sub> (% vol)</b>
<b>21% steam</b>	21	35	44
<b>35 % steam</b>	35	35	30

184

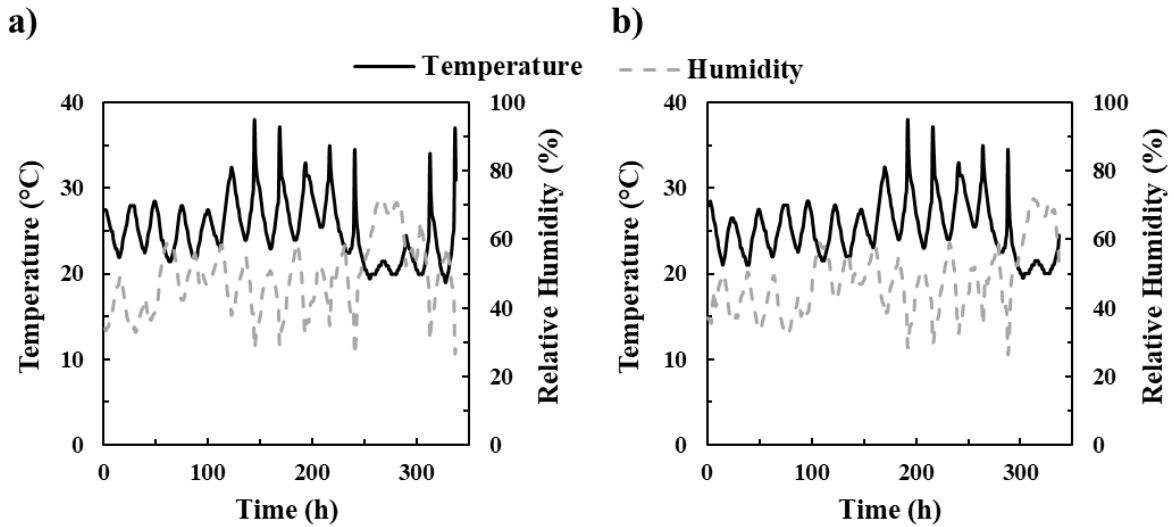
### 185 2.3 Material preparation and characterisation

186 Longcal limestone, supplied by Longcliffe Ltd., which has been used in our recent studies [46]  
187 as a typical natural source of high-purity calcium carbonate, contains minimum of 98.25%  
188 CaCO<sub>3</sub>. The limestone was sieved to the desired particle size range (250 to 500  $\mu\text{m}$ ). A Pyris  
189 1 TGA (Perkin Elmer) was used to determine the levels of hydration and carbonation of the  
190 samples after calcination in the BFB calciner as well as after their exposure to ambient air for  
191 DAC, by means of heating them to 900 °C at 30 °C/min in N<sub>2</sub>. Also, the morphology of samples  
192 was characterised by a Philips XL30ESEM Scanning Electron Microscope (SEM) using an  
193 accelerating voltage of 20 keV. The samples were coated with gold before analysis in order to  
194 avoid electrostatic charging.

### 195 2.4 Direct air capture (DAC) tests

196 For the DAC experiments, the materials calcined in the BFB calciner were exposed to air by  
197 placing them in stainless steel trays (45 cm x 35 cm), forming a thin layer (~3 mm). Samples  
198 from the trays were taken after 7 and 14 days for characterisation by the TGA in order to assess  
199 their hydration and carbonation extents, i.e., DAC performance. The samples were denoted as  
200 CaO-DAC-21 and CaO-DAC-35, referring to 21% and 35% vol steam in the calciner,  
201 respectively. The ambient air temperature and humidity were continuously monitored through

202 the DAC experiment and can be found in Figure 2. It can be seen that the temperature and  
203 humidity profiles for both experiments are very similar with cyclic fluctuations through each  
204 day.



205

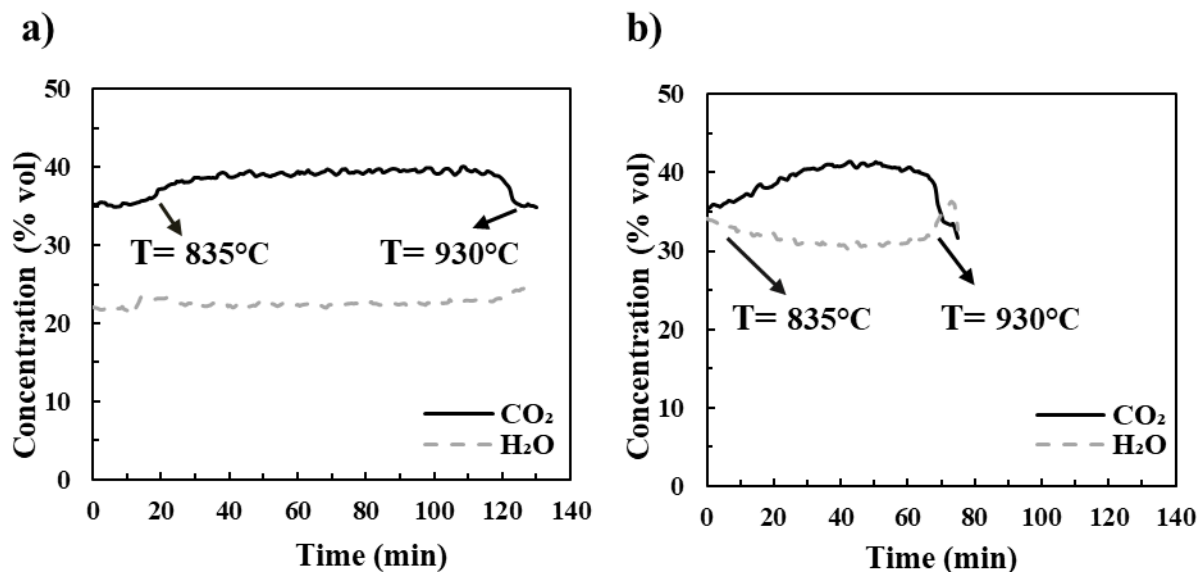
206 Figure 2: Temperature and humidity profiles for a) CaO-DAC-21, and b) CaO-DAC-35 tests.

### 207 3 Results and discussion

#### 208 3.1 Calcination in BFB calciner

209 During the calcination tests, the initial  $\text{CO}_2$  partial pressure was the same for both experiments  
210 and the material inventory was maintained the same in order to enable direct comparison of the  
211 temperature profiles and reaction times. The reaction started at near equilibrium temperature  
212 as the material decreased the temperature of the calciner substantially when introduced. The  
213 heat produced by combustion of natural gas was utilised for the endothermic calcination  
214 process. The  $\text{CO}_2$  and steam concentrations measured during the pilot-plant calcination  
215 experiments with 21% and 35% vol steam are presented in Figure 3. It can be seen that the  $\text{CO}_2$   
216 concentration increases when the calcination temperature is reached due to  $\text{CO}_2$  being released  
217 as  $\text{CaCO}_3$  decomposes. When calcination was completed, the  $\text{CO}_2$  concentration decreased to  
218 the initial value. The calcination started at 835 °C for both experiments, as expected, since the

219 CO<sub>2</sub> partial pressure was the same. Therefore, the effect of the steam concentration on the  
220 calcination temperature was negligible under these conditions and on the onset of calcination.  
221 The key difference between both experimental campaigns was the duration of the calcination  
222 reaction, which dropped from 110 min for 21% vol steam to 70 min for 35% vol steam.  
223 Therefore, higher steam concentration increases the rate of the calcination reaction. These  
224 results imply that steam present during calcination has a catalytic role, which has been  
225 suggested previously and is in agreement with the literature data [17]. The mechanism of this  
226 catalytic effect can be related to the fact that calcination is a reversible reaction and adsorption  
227 of H<sub>2</sub>O molecules at the active sites of limestone during calcination weakens the CaO-CO<sub>2</sub>  
228 bounds [17]. These findings also imply practical benefits of steam presence at elevated  
229 concentrations, such as those when the SOFC afterburner gas is used for calcination, and in  
230 addition to lowering the CO<sub>2</sub> partial pressure, steam acts as a catalyst and can significantly  
231 reduce required residence time of the material in the BFB calciner, which increases its capacity  
232 and efficiency. However, it should be noted that steam is believed to affect the attrition and  
233 elutriation rates of the material in the fluidised bed. It has been suggested that exposure to  
234 steam during calcination weakens particle structure and enhances particle attrition [27]. This is  
235 caused by the chemical effect of high steam concentrations on the CaO structure [19]. On the  
236 other hand, steam injection has shown other benefits when injected in the calciner, such as the  
237 improvement of the multicycle CO<sub>2</sub> carrying activity of lime-based materials using standard  
238 CaL conditions [11,12]. Finally, by using simulated SOFC gas for calcination, this study  
239 demonstrates the technical feasibility of the integrated SOFC-calciner process proposed for  
240 power generation with simultaneous lime production for DAC.



241

242 Figure 3: Gas concentrations measured by FTIR at outlet of the BFB calciner for a) 21% vol  
 243 steam, and b) 35% vol steam.

### 244 3.2 Direct air capture (DAC) results

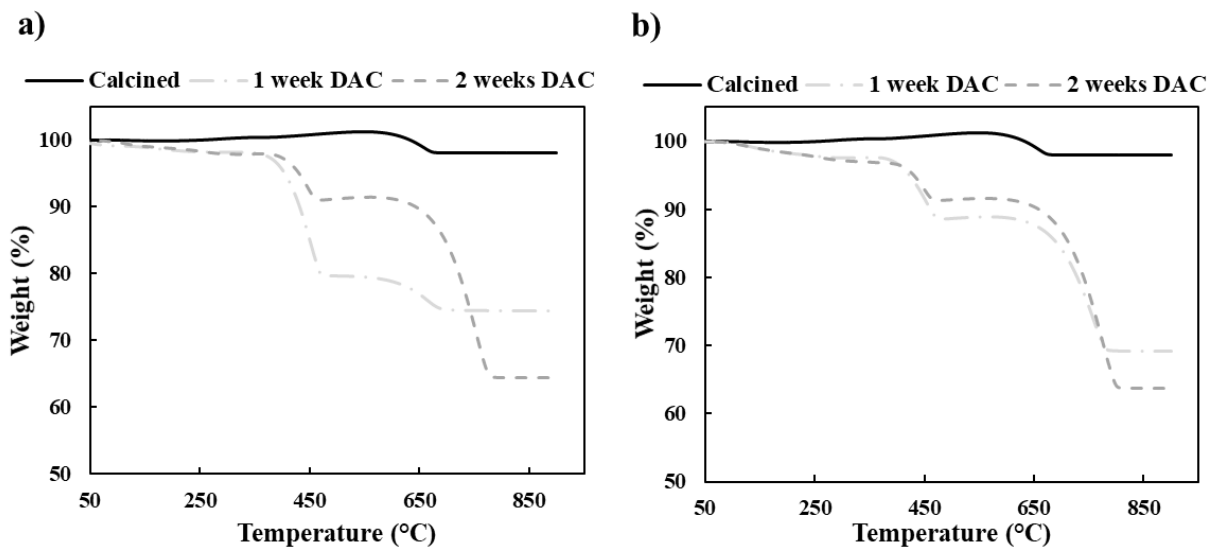
245 After each pilot-plant calcination, the materials were tested in the TGA to assess the  
 246 completeness of the calcination and possible hydration and/or re-carbonation during the  
 247 cooling down step and discharging the inventory of the calciner. The TGA results from the  
 248 calcined samples are shown in Figure 4 (solid lines), and the hydration and carbonation  
 249 conversions are presented in Table 2. It can be seen that both samples were almost completely  
 250 calcined after each test, regardless of the steam concentration, which was expected based on  
 251 the CO<sub>2</sub> profiles presented in Figure 3, and there was no significant difference between the  
 252 TGA decomposition curves. The small mass loss observed between 550-700 °C can be  
 253 attributed to ambient carbonation of the CaO-based sorbent during the discharge process and/or  
 254 presence of some non-calcined material.

255 After the pilot-plant calcination tests, the samples were exposed to air in order to investigate  
 256 their hydration and carbonation conversions, i.e., DAC performance, over a prolonged  
 257 duration. In Figure 4a, the weight losses for CaO-DAC-21 sample during heating to 900 °C are

258 shown. These data correspond to the DAC capacity of the material after 7 and 14 days. It can  
259 be seen that during the first week the material was mainly hydrated by moisture from the air  
260 which reacts with the CaO surface. Some carbonation can be also seen during that period, but  
261 it was negligible when compared to the hydration conversion. The corresponding TGA profile  
262 is shown for CaO-DAC-35 sample in Figure 4b. It appears that the sample which was exposed  
263 to the higher steam concentration during calcination carbonates faster at the beginning, i.e.,  
264 carbonation conversions after 7 days are 8% and 36% for CaO-DAC-21 and CaO-DAC-35,  
265 respectively. However, after 14 days the carbonation conversions were very similar at around  
266 53-55%. This suggests that steam present during calcination has a positive effect on the  
267 material at the beginning of the air capture process, increasing the rate of carbonation when the  
268 steam concentration was higher. It should be noted that DAC by lime, as considered in this  
269 study, is a long process that takes weeks/months if not aided by forcing air through the material.  
270 Therefore, it may not be economically feasible to increase the steam concentration in the  
271 calcination gas for a rise in reaction rate during a short period of DAC. However, depending  
272 on the application of this technology, namely, the source of the fluidising calcination gas, the  
273 gas can be inherently rich in steam, which is the case for the integrated SOFC calciner. In this  
274 case, the re-carbonation during DAC would be faster during the initial stages, which can enable  
275 more frequent recycling of the material to the calciner, depending on other thermodynamic and  
276 economic parameters of the proposed DAC process.

277 It can be inferred that a higher steam concentration during the calcination reaction aids the air  
278 capture performance of the material. However, it has been previously suggested that steam  
279 enhances sorbent sintering during calcination [23]. This is believed to be caused by the  
280 formation of OH<sup>-</sup> ions, which support the growth of CaO crystals causing the surface area to  
281 decrease. However, the same phenomenon can favour the increase of the particle's mean pore  
282 size and mitigate the reactivity decay over the cycles [11,12]. Therefore, the carbonation may

283 be promoted by improved accessibility of CaO in the particles. As the steam addition during  
 284 the reaction affects sorbent morphology, the pore structure is believed to be more stable [47].  
 285 This, perhaps, removes the delay in the first stage of the carbonation reaction (kinetically-  
 286 controlled) and raises the reaction rate in the second stage of the reaction (diffusion-controlled).  
 287 All of these effects are expected to increase the carbonation kinetics of CaO. However, it should  
 288 be noted that previous studies have claimed that steam has a greater impact on sorbent reactivity  
 289 when injected during carbonation, while a less significant effect has been found when steam is  
 290 injected during calcination [12].



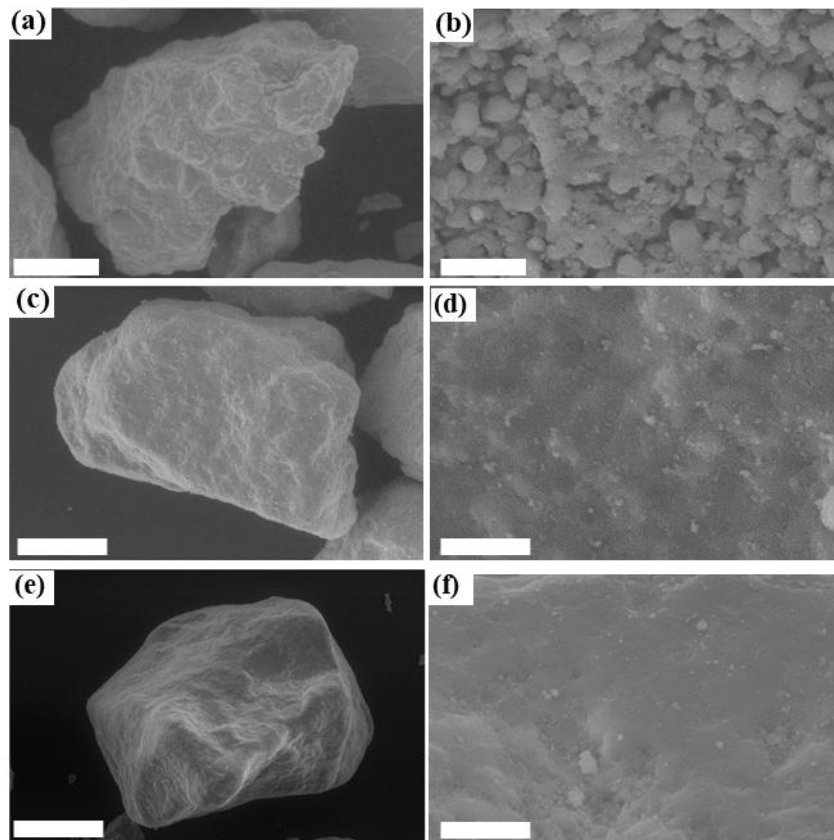
291  
 292 Figure 4: Re-carbonation experiments for: a) CaO-DAC-21, and b) CaO-DAC-35 calcined  
 293 materials. Note:  $X_h$  and  $C_{carb}$  refer to hydration and carbonation conversions, respectively.

294 Table 2: Hydration and carbonation conversions for DAC experiments\*

Sample	$X_h$ (%)	$X_{carb}$ (%)
CaO-DAC-21-1week	79	8
CaO-DAC-21-2week	34	53
CaO-DAC-35-1week	41	36
CaO-DAC-35-2week	31	55

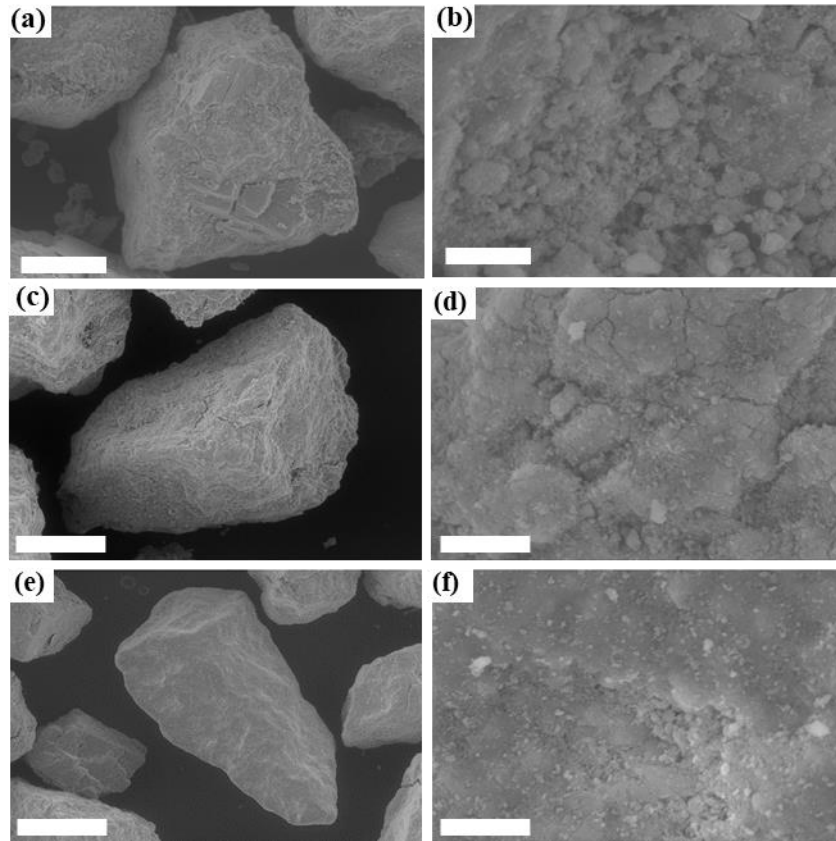
295 \* Note:  $X_h$  and  $X_{carb}$  refer to hydration and carbonation conversions, respectively

296 Figures 5 and 6 show selected SEM images of the CaO-based materials calcined under different  
297 steam concentration conditions, as well as corresponding samples after exposure to air for  
298 prolonged durations. It can be seen that the increase in steam concentration during the  
299 calcination aids the development of a more resistant structure due to larger pores and a more  
300 open pore structure. These results are in agreement with the previous findings by Donat et al.  
301 [11] and Coppola et al. [48]. It can also be observed how the morphology of the material  
302 changes during hydration/re-carbonation by air. A very porous structure is characteristic for  
303 the calcines presented in Figures 5b and 6b, changing to a compact structure presented in  
304 Figures 5f and 6f due to the formation of a carbonate layer which fills the pores.



305  
306 Figure 5: SEM images of particles after the 21% vol steam calcination test and exposure to air:  
307 a) and b) calcined material; and material after c) and d) one week of re-carbonation, and e) and  
308 f) two weeks of re-carbonation. The bars are 250  $\mu\text{m}$  for a), c), and e); and 10  $\mu\text{m}$  for b), d) and  
309 f).





310

311 Figure 6: SEM images of particles after the 35% vol steam calcination test and exposure to air:  
 312 a) and b) calcined material; and material after c) and d) one week of re-carbonation; and e) and  
 313 f) two weeks of re-carbonation. The bars are 250  $\mu\text{m}$  for a), c), and e); and 10  $\mu\text{m}$  for b), d) and  
 314 f).

315 The results presented in this paper clearly demonstrated technical feasibility of the calciner  
 316 component of the integrated SOFC-calciner concept for lime production. Both catalytic role of  
 317 stem and reducing calcination temperature due to lowering partial pressure of  $\text{CO}_2$  plays a  
 318 crucial role in further development of the concept considering that steam is inherently present  
 319 in the system. This means higher efficiency of the technology, and concentrated stream of  $\text{CO}_2$   
 320 is easily produced after steam condensation. Importantly, produced lime has superior  
 321 morphology and performance in removing  $\text{CO}_2$  from air when exposed to the ambient  
 322 conditions. Therefore, the concept is carbon-negative ready, and demonstration of the calciner  
 323 component of the concept is a driver for the further development of the concept, considering

324 that produced lime can be sold in market, but in the case it is needed, produced lime can be  
325 used to remove CO<sub>2</sub> from air.

#### 326 **4 Conclusions**

327 Different steam-rich conditions (21% vol and 35% vol) were tested for the calcination of  
328 limestone at pilot scale using a bubbling fluidised bed (BFB) calciner, with 35% vol CO<sub>2</sub>, and  
329 balance N<sub>2</sub>, in order to evaluate the effect of steam and subsequent DAC performance of the  
330 calcined materials. It was found that steam had a significant effect on the duration of  
331 calcination, reducing carbonation time from 110 min in 21% steam to 70 min in 35% steam.  
332 However, the onset calcination temperature seemed unaltered when varying the steam  
333 concentration (around 835 °C). This suggests a catalytic effect of steam, which aids calcination  
334 near the equilibrium temperature. After calcination, the lime material was exposed to air in  
335 order to investigate its potential for DAC. It was found that the materials carbonated fairly  
336 quickly, exceeding 50% carbonation conversion after 14 days, which is of practical interest for  
337 utilisation at industrial scale. This also implies that the high levels of steam present during  
338 calcination promote the DAC performance of CaO-based materials. Moreover, the increased  
339 steam concentration during the calcination has a more positive effect in the first stage of the  
340 subsequent re-carbonation under ambient conditions. This is believed to be due to the fact that  
341 steam present during calcination alters the porous structure of lime, making it more stable and  
342 with larger pores. Therefore, CO<sub>2</sub> would encounter lower diffusion resistance when it reacts  
343 with CaO in the lime particles. In addition to further highlighting the effects of steam on  
344 calcination of limestone, these results also demonstrate the technical feasibility of calcination  
345 in a steam-rich gas stream such as that from a SOFC and suitability of the calcines for DAC,  
346 with a potential for power generation with negative carbon emissions.

## 347 **Acknowledgments**

348 This work is part of the “Balanced Energy Network” project supported by InnovateUK  
349 Integrated Supply Chains for Energy Systems Grant (InnovateUK reference: 102624). The  
350 consortium consists of ICAX Ltd., London South Bank University, Terra Firma Ground  
351 Investigation Ltd., Upside Energy Ltd., Mixergy Ltd., Origen Power Ltd., and Cranfield  
352 University. The authors would like to thank Mr Howard Smith for his kind help and support  
353 during this work. Longcliffe Quarries Ltd is acknowledged for the supply of its Longcal  
354 limestone.

## 355 **References**

- 356 [1] Tollefson J. The 2°C dream. *Nature* 2015;527:436–8.  
357 doi:10.1016/j.ecoenv.2014.01.038.
- 358 [2] Fajardy M, Chiquier S, Mac Dowell N. Investigating the BECCS resource nexus:  
359 delivering sustainable negative emissions. *Energy Environ Sci* 2018.
- 360 [3] IEA. *Tracking Clean Energy Progress*. Paris, France: 2017.
- 361 [4] Aminu MD, Nabavi SA, Rochelle CA, Manovic V. A review of developments in carbon  
362 dioxide storage. *Appl Energy* 2017;208:1389–419.
- 363 [5] Buck HJ. Rapid scale-up of negative emissions technologies: social barriers and social  
364 implications. *Clim Change* 2016;139:155–67.
- 365 [6] Sanchez DL, Callaway DS. Optimal scale of carbon-negative energy facilities. *Appl*  
366 *Energy* 2016;170:437–44.
- 367 [7] Smith P. Soil carbon sequestration and biochar as negative emission technologies. *Glob*  
368 *Chang Biol* 2016;22:1315–24.
- 369 [8] Edmonds J, Luckow P, Calvin K, Wise M, Dooley J, Kyle P, et al. Can radiative forcing  
370 be limited to 2.6 Wm<sup>-2</sup> without negative emissions from bioenergy and CO<sub>2</sub> capture and  
371 storage? *Clim Change* 2013;118:29–43.
- 372 [9] Hanak DP, Michalski S, Manovic V. From post-combustion carbon capture to sorption-  
373 enhanced hydrogen production: A state-of-the-art review of carbonate looping process  
374 feasibility. *Energy Convers Manag* 2018;177:428–52. doi:10.1016/j.enconman.2018.09.058.
- 375 [10] Markewitz P, Kuckshinrichs W, Leitner W, Linssen J, Zapp P, Bongartz R, et al.  
376 Worldwide innovations in the development of carbon capture technologies and the utilization  
377 of CO<sub>2</sub>. *Energy Environ Sci* 2012;5:7281–305.

- 378 [11] Donat F, Florin NH, Anthony EJ, Fennell PS. Influence of high-temperature steam on  
379 the reactivity of CaO sorbent for CO<sub>2</sub> capture. *Environ Sci Technol* 2012;46:1262–9.
- 380 [12] Champagne S, Lu DY, Macchi A, Symonds RT, Anthony EJ. Influence of steam  
381 injection during calcination on the reactivity of CaO-based sorbent for carbon capture. *Ind Eng*  
382 *Chem Res* 2013;52:2241–6.
- 383 [13] Symonds RT, Lu DY, Manovic V, Anthony EJ. Pilot-scale study of CO<sub>2</sub> capture by  
384 CaO-based sorbents in the presence of steam and SO<sub>2</sub>. *Ind Eng Chem Res* 2012;51:7177–84.
- 385 [14] Manovic V, Anthony EJ. Carbonation of CaO-based sorbents enhanced by steam  
386 addition. *Ind Eng Chem Res* 2010;49:9105–10.
- 387 [15] Symonds RT, Lu DY, Hughes RW, Anthony EJ, Macchi A. CO<sub>2</sub> capture from  
388 simulated syngas via cyclic carbonation/calcination for a naturally occurring limestone: pilot-  
389 plant testing. *Ind Eng Chem Res* 2009;48:8431–40.
- 390 [16] Baker EH. The calcium oxide–carbon dioxide system in the pressure range 1–300  
391 atmospheres. *J Chem Soc* 1962:464–70.
- 392 [17] Wang Y, Thomson WJ. The effects of steam and carbon dioxide on calcite  
393 decomposition using dynamic X-ray diffraction. *Chem Eng Sci* 1995;50:1373–82.
- 394 [18] Asano K, Yamaguchi Y, Fujimoto K, Ito S. Reactivity of carbonates in superheated  
395 steam under atmospheric pressure. *Key Eng Mater* 2014;617.
- 396 [19] MacIntire WH, Stansel TB. Steam catalysis in calcinations of dolomite and limestone  
397 fines. *Ind Eng Chem* 1953;45:1548–55.
- 398 [20] Berger EE. Effect of steam on the decomposition of limestone<sup>1</sup>. *Ind Eng Chem*  
399 1927;19:594–6.
- 400 [21] Wang Y, Lin S, Suzuki Y. Experimental study on CO<sub>2</sub> capture conditions of a fluidized  
401 bed limestone decomposition reactor. *Fuel Process Technol* 2010;91:958–63.
- 402 [22] Stanmore BR, Gilot P. Calcination and carbonation of limestone during thermal cycling  
403 for CO<sub>2</sub> sequestration. *Fuel Process Technol* 2005;86:1707–43.
- 404 [23] Borgwardt RH. Calcium oxide sintering in atmospheres containing water and carbon  
405 dioxide. *Ind Eng Chem Res* 1989;28:493–500.
- 406 [24] Agnew J, Hampartsoumian E, Jones JM, Nimmo W. The simultaneous calcination and  
407 sintering of calcium based sorbents under a combustion atmosphere. *Fuel* 2000;79:1515–23.
- 408 [25] Anderson PJ, Horlock RF, Avery RG. Some effects of water vapour during the  
409 preparation and calcination of oxide powders. *Proc. Brit. Ceram. Soc*, vol. 3, 1965, p. 33–42.
- 410 [26] Fierro V, Adánez J, Garcia-Labiano F. Effect of pore geometry on the sintering of Ca-  
411 based sorbents during calcination at high temperatures. *Fuel* 2004;83:1733–42.
- 412 [27] Coppola A, Allocca M, Montagnaro F, Scala F, Salatino P. The effect of steam on CO<sub>2</sub>  
413 uptake and sorbent attrition in fluidised bed calcium looping: The influence of process  
414 conditions and sorbent properties. *Sep Purif Technol* 2017;189:101–7.  
415 doi:10.1016/j.seppur.2017.08.001.

- 416 [28] Ortiz C, Chacartegui R, Valverde JM, Alovio A, Becerra JA. Power cycles integration  
417 in concentrated solar power plants with energy storage based on calcium looping. *Energy*  
418 *Convers Manag* 2017;149:815–29.
- 419 [29] Yuan Y, Li Y, Duan L, Liu H, Zhao J, Wang Z. CaO/Ca(OH)<sub>2</sub> thermochemical heat  
420 storage of carbide slag from calcium looping cycles for CO<sub>2</sub> capture. *Energy Convers Manag*  
421 2018;174:8–19.
- 422 [30] Lackner K, Ziock HJ, Grimes P. Carbon dioxide extraction from air: Is it an option?  
423 1999.
- 424 [31] Nikulshina V, Gebald C, Steinfeld A. CO<sub>2</sub> capture from atmospheric air via consecutive  
425 CaO-carbonation and CaCO<sub>3</sub>-calcination cycles in a fluidized-bed solar reactor. *Chem Eng J*  
426 2009;146:244–8.
- 427 [32] Hanak DP, Jenkins BG, Kruger T, Manovic V. High-efficiency negative-carbon  
428 emission power generation from integrated solid-oxide fuel cell and calciner. *Appl Energy*  
429 2017;205:1189–201. doi:10.1016/j.apenergy.2017.08.090.
- 430 [33] Gür TM, Homel M, Virkar A V. High performance solid oxide fuel cell operating on  
431 dry gasified coal. *J Power Sources* 2010;195:1085–90.
- 432 [34] Alexander BR, Mitchell RE, Gür TM. Experimental and modeling study of biomass  
433 conversion in a solid carbon fuel cell. *J Electrochem Soc* 2012;159:B347–54.
- 434 [35] Lee AC, Li S, Mitchell RE, Gür TM. Conversion of solid carbonaceous fuels in a  
435 fluidized bed fuel cell. *Electrochem Solid-State Lett* 2008;11:B20–3.
- 436 [36] Liu M, Choi Y, Yang L, Blinn K, Qin W, Liu P, et al. Direct octane fuel cells: A  
437 promising power for transportation. *Nano Energy* 2012;1:448–55.
- 438 [37] Wachsman ED, Marlowe CA, Lee KT. Role of solid oxide fuel cells in a balanced  
439 energy strategy. *Energy Environ Sci* 2012;5:5498–509.
- 440 [38] De Lorenzo G, Fragiaco P. Energy analysis of an SOFC system fed by syngas.  
441 *Energy Convers Manag* 2015;93:175–86.
- 442 [39] Inui Y, Urata A, Ito N, Nakajima T, Tanaka T. Performance simulation of planar SOFC  
443 using mixed hydrogen and carbon monoxide gases as fuel. *Energy Convers Manag*  
444 2006;47:1738–47.
- 445 [40] Zink F, Lu Y, Schaefer L. A solid oxide fuel cell system for buildings. *Energy Convers*  
446 *Manag* 2007;48:809–18.
- 447 [41] Gür TM. Comprehensive review of methane conversion in solid oxide fuel cells:  
448 prospects for efficient electricity generation from natural gas. *Prog Energy Combust Sci*  
449 2016;54:1–64.
- 450 [42] Hanak DP, Manovic V. Combined heat and power generation with lime production for  
451 direct air capture *Energy Convers Manag* 2018;160:455-66.
- 452 [43] Nabavi SA, Erans M, Manovic V. Demonstration of a kW-Scale SOFC-integrated  
453 calciner for simultaneous power generation and lime production. 2019, under review

- 454 [44] Erans M, Jeremias M, Manovic V, Anthony EJ. Operation of a 25 kWth calcium  
455 looping pilot-plant with high oxygen concentrations in the calciner. *Journal of Visualised*  
456 *Experiments* 2017;128:e56112.
- 457 [45] Alonso M, Arias B, Fernández JR, Bughin O, Abanades C. Measuring attrition  
458 properties of calcium looping materials in a 30 kW pilot plant. *Powder Technol* 2018;336:273–  
459 81.
- 460 [46] Erans M, Jeremias M, Zheng L, Yao JG, Blamey J, Manovic V, et al. Pilot testing of  
461 enhanced sorbents for calcium looping with cement production. *Appl Energy* 2018;225:392–  
462 401. doi:10.1016/j.apenergy.2018.05.039.
- 463 [47] Phalak N, Deshpande N, Fan L-S. Investigation of high-temperature steam hydration  
464 of naturally derived calcium oxide for improved carbon dioxide capture capacity over multiple  
465 cycles. *Energy & Fuels* 2012;26:3903–9.
- 466 [48] Coppola A, Salatino P, Montagnaro F, Scala F. Hydration-induced reactivation of spent  
467 sorbents for fluidized bed calcium looping (double looping). *Fuel Process Technol*  
468 2014;120:71–8.
- 469